A24

Journal of chemical & engineering data

Article

pubs.acs.org/jced

# Adsorption of Phenol from Aqueous Solution on a Low-Cost Activated Carbon Produced from Tea Industry Waste: Equilibrium, Kinetic, and Thermodynamic Study

Ali Gundogdu,*[,†] Celal Duran,[‡] H. Basri Senturk,[‡] Mustafa Soylak,[§] Duygu Ozdes,[∥] Huseyin Serencam,[⊥] and Mustafa Imamoglu[#]

[†]Department of Food Engineering, Faculty of Engineering, Gumushane University, 29100 Gumushane, Türkiye

[‡]Department of Chemistry, Faculty of Sciences, Karadeniz Technical University, 61080 Trabzon, Türkiye

[§]Department of Chemistry, Faculty of Sciences, Erciyes University, 38039 Kayseri, Türkiye

[∥]Gumushane Vocational School, Gumushane University, 29100 Gumushane, Türkiye

[⊥]Department of Food Engineering, Faculty of Engineering, Bayburt University, 69000 Bayburt, Türkiye

[#]Department of Chemistry, Faculty of Arts & Sciences, Sakarya University, 54187 Sakarya, Türkiye

**ABSTRACT:** The ability of activated carbon which was produced by chemical activation using zinc chloride from tea industry wastes (TIWAC) to adsorb phenol molecules from aqueous solution was tested by equilibrium, kinetic, and thermodynamic parameters. Phenol adsorption on TIWAC took place with a high yield at pH values in the range 4 to 8. The optimum contact period was observed as 4.0 h and from the adsorption graphs plotted as a function of time; it was established that phenol adsorption on TIWAC conformed more to a pseudosecond-order kinetic model. Additionally, it was determined that the adsorption rate is controlled by intraparticle diffusion as well as film diffusion. It was established that phenol adsorption on TIWAC can be better defined by the Langmuir adsorption model and its adsorption capacity was 142.9 mg·g$^{-1}$ from the linear Langmuir equation. Temperature had an adverse effect on adsorption yield, and hence, the adsorption process was exothermic in our case. Moreover, increasing electrolyte concentration in the medium has a positive effect on adsorption yield. From the data obtained, it was concluded that the removal of phenol from aqueous solution by TIWAC produced from tea industry wastes with a very low cost took place with an extremely high performance.

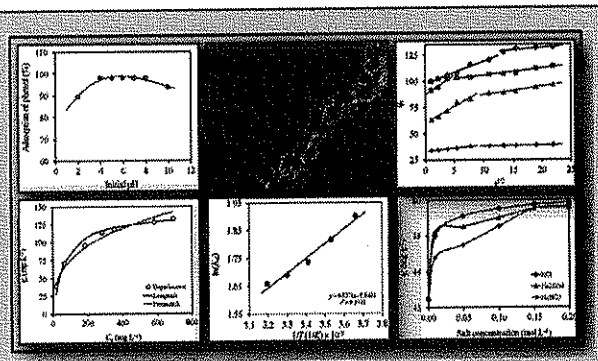

## 1. INTRODUCTION

Phenol is an important toxicant which is among the topmost toxic chemicals. In water, it manifests itself by causing a noticeable unpleasant taste and odor change during chlorinating water even though its concentration is at ppm level and even less than that. Since phenols are protoplasmic toxins, they are harmful for all live cell types. Drinking water containing phenol may cause severe renal insufficiency, convulsions, and even death. Most chlorophenols are corrosive to skin and eye. Especially, coal distillation and organic synthesis waste flows of coal entities have large amounts of phenol and its derivatives. Phenolic compounds are also contained in wastewater from pulp and paper bleaching facilities, resin, pesticide, insecticide, paint, and solvent industries. Chlorinating wastewater containing phenol for disinfection purposes causes the formation of extremely toxic chlorophenols. Also, another source of phenols in water is plants in nature. Phenolic species are directly or indirectly transmitted to water from volatile compounds emitted by the plants to the atmosphere.[1−3]

Phenolic compounds can be removed by physical, chemical, and/or biological methods. One of the methods used in the treatment of wastewater containing medium level phenolic contamination is biological treatment (lagoons, vented stabilization pools, trickling filters, and active sludge systems) pools, and the other is adsorption.[4] The adsorption method is effectively used in the removal of phenol and its derivatives in undesirable concentrations in wastewater of petrol refineries, coke, drug, paint, plastic, insecticide, pesticide, and paper industries.

Most of the adsorption studies in which good results were obtained have been the studies with activated carbons with a large surface area. The removal of phenol by adsorption on activated carbons is the most efficient and the most frequently used method compared to other processes such as aerobic and

Received: June 4, 2012
Accepted: August 15, 2012
Published: August 27, 2012

   dx.doi.org/10.1021/je300597u | J. Chem. Eng. Data 2012, 57, 2733−2743

anaerobic biodegradation, oxidation with ozone, and use of ion exchange resins.[5] The adsorption ability of activated carbons is a result of their high surface area, microporous structure, and high level surface activity. Therefore, activated carbons are exploited to purify harmful components from gas and liquid solutions, remove their colors and odors, remove excess chlorine, separate and concentrate for quantitative recovery, filter, remove, or modify purposes.[6]

Many available low-cost raw materials with a high carbon content, such as agricultural byproduct, residues, or wastes, can be used in the production of activated carbon.[7,8] In this study, activated carbon was produced from wastes generated by the black tea production industry. Turkey's Eastern Black Sea Region is one of the leading countries producing black tea (*Camellia sinesis*). Therefore, tonnes of wastes are generated during the processing of green tea leaves. These wastes are not used in any industrial area and are most probably exploited as fertilizers. By producing activated carbon from these wastes, not only their risk of causing an environmental problem is eliminated, but also they will be regained by economy. Moreover, this study will be given a new meaning by the fact that the activated carbons produced will be used to dispose of other environmental pollution.

The production of activated carbon takes place in two steps: carbonization and activation. Carbonization is the pyrolysis of raw material at (500 to 1000) °C in an $N_2$ atmosphere to remove noncarbonaceous elements. Activation is a procedure which can be applied in two ways being physical or chemical and ensures that the precursor has a porous structure, hence a very large surface area. Thus, an adsorbent with highly developed adsorption ability is obtained. In physical activation, water vapor or $CO_2$, in chemical activation, and chemicals such as $ZnCl_2$, $H_3PO_4$, $H_2SO_4$, $HNO_3$, KOH, and $K_2CO_3$ are used as activating agents.[9−11] Zinc chloride was used as a chemical activation agent in this study for the production of activated carbon.

In this study, the ability of the activated carbon obtained from tea industry wastes (TIWAC) by chemical activation using zinc chloride to remove phenol molecules from aqueous solution by adsorption was tested by various analytical parameters in terms of equilibrium, kinetics, and thermodynamics.

## 2. MATERIALS AND METHOD

**2.1. Preparation of Activated Carbon.** Tea industry wastes (TIW) were procured from tea factories in the town of Of, in the province of Trabzon-Turkey. First tea wastes were dried and ground, and 20 g of tea wastes of (125 to 300) $\mu$m and 20 g of $ZnCl_2$ were mixed (precursor/activating agent ratio, 1:1). A portion of 150 mL of distilled water was added to the mixture, and the mixture was allowed to stand for 1 day. At the end of one day extra solution was removed by filtration, and the mixture was put into a stainless steel reactor. The reactor was placed in a high temperature furnace (Nüve MF 100), and its temperature was set to 700 °C under nitrogen atmosphere. The nitrogen flow rate was set to approximately 100 mL·min$^{-1}$. The heating procedure was started at room temperature and increased to 700 °C in approximately 80 min, and the mixture was pyrolized. Carbonization procedure was maintained for 4 h in total, and at the end of the procedure, the reactor was cooled down to room temperature under nitrogen atmosphere. The resultant activated carbon (TIWAC) was boiled in 2 M HCl, and any impurities in its content were removed. Then, it was filtered in vacuum filtration setup; treatment with HCl was repeated twice, and the resultant TIWAC was thoroughly washed with distilled water until the filtrate contains no more chloride. Finally, TIWAC was dried at 105 °C for 4 h and kept in a desiccator.[12−14]

**2.2. Characterization of TIWAC.** Proximate analyses were performed according to ASTM D2854-96 (2004) and ASTM D5832-98 (2003), and elemental analyses were performed by using a LECO CHNS-932 elemental analyzer.[15,16]

Surface characterization analyses were performed by $N_2$ adsorption at −196 °C using Micromeritics TriStar 3000 instrument. BET (Brunauer−Emmett−Teller) surface areas ($S_{BET}$), micropore areas ($S_{micro}$), and total micropore volumes ($V_{total}$) were calculated from $N_2$ adsorption isotherms.

The methylene blue number of TIWAC was determined by agitating 20 mg of TIWAC with methylene blue coloring agent of 1000 mg·L$^{-1}$ for 12 h, followed by analyzing the filtrate by UV−vis spectrometer,[17] whereas the iodine number was determined by treating 0.2 g of TIWAC with 40 mL of 0.1 N iodine solution, followed by titrating the filtrate with 0.1 N standardized thiosulfate solution for the amount of iodine left unadsorbed in the filtrate.[18]

SEM micrographs (by JEOL/JSM-6335F scanning electron microscope) and IR spectra (by Perkin-Elmer 1600 FT-IR spectrophotometer) were obtained both before and after phenol adsorption of TIWAC.

**2.3. Adsorption Tests.** The batch technique was applied in adsorption experiments. A sample of 30 mg of TIWAC was weighed in a series of capped polypropylene centrifuge tubes of 15 mL. Individual 10 mL solutions were added to them from 0.1 mol·L$^{-1}$ $HNO_3$ and/or 0.1 mol·L$^{-1}$ NaOH, and phenol solutions of (100 to 1000) mg·L$^{-1}$ with a pH adjusted to 6.0, and tube contents were agitated at 400 rpm for 4.0 h on a mechanical agitator. Next, tube contents were filtrated through 0.45 $\mu$m nitrocellulose membrane (Sartorius Stedim Biotech, GmbH). Phenol concentrations left unadsorbed in the solutions were determined by a UV−vis spectrophotometer (double-beam Unicam UV-2) at a wavelength of 269 nm.

Each experiment was carried out in minimum triplicate, and the average values were presented as results. By the courtesy of the unadsorbed phenol concentration in the solution, the amount of phenol adsorbed by 1 g of TIWAC was calculated in mg·g$^{-1}$ by the following formula:

$$q_e = \frac{(C_o - C_e)\cdot V}{m} \quad (1)$$

The percentage of adsorption was calculated by the following formula:

$$\text{adsorption}(\%) = \frac{C_o - C_e}{C_o}\cdot 100 \quad (2)$$

where $q_e$ is the amount of phenol adsorbed by 1 g TIWAC (mg·g$^{-1}$), $C_o$ is the initial phenol concentration (mg·L$^{-1}$), $C_e$ is the phenol concentration unadsorbed in the solution at equilibrium (mg·L$^{-1}$), $V$ is the volume of phenol solution (mL), and $m$ is the amount of TIWAC (g).

**2.4. Adsorption Kinetics.** *2.4.1. Pseudofirst-Order Kinetic Model.* Pseudofirst-order kinetic model was set forth by Lagergren in 1898.[19] This model is not applicable for a total adsorption period for many instances. It can be generally used for the first minutes of adsorption procedure in other words for

the periods before reaching equilibrium.[20] This adsorption rate can be expressed by the equation,

$$\frac{dq}{dt} = k_1(q_e - q) \tag{3}$$

If the equation is integrated with limit terms in which $t = 0$, $q = 0$, and $t = t$, $q = q_t$, the equation takes the form;

$$\ln(q_e - q_t) = \ln q_e - k_1 t \tag{4}$$

where $q_e$ (mg·g$^{-1}$) and $q_t$ (mg·g$^{-1}$) show the amount of adsorbate adsorbed on the adsorbent at equilibrium and at time $t$, respectively. $k_1$ (min$^{-1}$) is pseudofirst-order rate constant. A plot of $\ln(q_e - q_t)$ versus $t$ is a line and gives information about whether this kinetic model is compatible with adsorption data. $q_e$ and $k_1$ can be obtained from the intercept and slope of the graph, respectively.

*2.4.2. Pseudosecond-Order Kinetic Model.* The pseudo-second-order kinetic model is another model used in the analysis of adsorption kinetic data. Contrary to the pseudofirst-order kinetic model, this model is compatible with the mechanism of rate-controlling step throughout the adsorption. The pseudosecond-order kinetic model is given by the following equation:[21]

$$\frac{dq_t}{dt} = k_2(q_e - q_t)^2 \tag{5}$$

When rearranged, it becomes;

$$\frac{t}{q_t} = \frac{1}{k_2 q_e^{\,2}} + \frac{t}{q_e} \tag{6}$$

$k_2$ (g·mg$^{-1}$·min$^{-1}$) is the second-order rate constant. If the plot of $t/q_t$ versus $t$ is a line, this line shows that kinetic data are compatible with the second-order kinetic model. $q_e$ and $k_2$ can be obtained from the slope and intercept of the graph, respectively.

*2.4.3. Intraparticle Diffusion Model.* The progress of adsorption can be monitored by the application of intraparticle diffusion model, and the rate-controlling step(s) can be determined. The intraparticle diffusion model is given by the following equation:[22]

$$q_t = k_{id} t^{1/2} + C \tag{7}$$

where $k_{id}$ (mg·g$^{-1}$·min$^{-1/2}$) is the intraparticle diffusion rate constant and $C$ (mg·g$^{-1}$) is a constant characterizing boundary layer thickness. $k_{id}$ and $C$ can be determined from the slope and intercept of a plot drawn between $q_t$ and $t^{1/2}$.

In a plot of $q_t$ versus $t^{1/2}$ multilinear correlation can be observed. The first sharp part in the line shows film diffusion or adsorption. The second part is a more advanced adsorption section, that is, where diffusion is the rate-controlling grade. The third part is the equilibrium section, and in this part, intraparticle diffusion starts to slow down because of the very low concentration of the substance remaining in the solution.[23] If the linear section in the second part, that is, the intercept point ($C$) of the line representing intraparticle diffusion goes through the origin, it is concluded that the adsorption rate-controlling step is only intraparticle diffusion. If not, it can be stated that adsorption rate is controlled by more than one mechanism.[24]

**2.5. Adsorption Isotherms.** *2.5.1. Langmuir Adsorption Isotherm.* According to the theory, any atoms or molecules moving toward active regions (functional groups) of a crystalline surface are deemed to be adsorbed on these regions. As such sites on the surface can only accommodate one atom or molecule, it is suggested that the adsorbed layer is a monomolecular layer and also active regions of the adsorbent form a homogeneous layer.[25]

A curvilinear Langmuir isotherm can be expressed by the following mathematical equation:

$$q_e = \frac{bC_e}{1 + bC_e} \tag{8}$$

The linear form of the equation is as follows:

$$\frac{C_e}{q_e} = \frac{C_e}{q_{max}} + \frac{1}{bq_{max}} \tag{9}$$

where $q_e$ is the amount of adsorbate adsorbed by 1 g of adsorbent (mg·g$^{-1}$), $q_{max}$ is the maximum single layer adsorption capacity (mg·g$^{-1}$), $C_e$ is the amount of adsorbate left unadsorbed in the solution at equilibrium (mg·L$^{-1}$), and $b$ is a constant related to free energy or adsorption enthalpy (L·mg$^{-1}$).

A plot of $C_e/q_e$ versus $C_e$ gives a linear graph and indicates compatibility of adsorption with the Langmuir model. $q_{max}$ and $b$ can be determined from the slope and intercept, respectively. $q_{max}$ gives the maximum adsorption capacity of the adsorbent. However, in the case of heterogeneous adsorption systems where monolayer adsorption takes place, the Langmuir isotherm cannot clearly describe the equilibrium state.

The $b$ constant is a constant depending on temperature and adsorption enthalpy with respect to the closeness of active sites on the adsorbent surface with each other.

Another important parameter of the Langmuir isotherm model is the term "$R_L$" which is a nondimensional constant and called as separation factor or equilibrium parameter, and it is represented by the following equation:[26]

$$R_L = \frac{1}{1 + bC_o} \tag{10}$$

where $C_o$ (mg·L$^{-1}$) expresses initial adsorbate concentration in aqueous solution. $b$ (L·mg$^{-1}$) is the Langmuir constant. The $R_L$ parameter gives important signs on the compatibility of adsorption for the selected adsorbent−adsorbate pair. There are four possibilities for the $R_L$ value:[26]

- In the case $0 < R_L < 1$, adsorption is favorable.
- In the case $R_L > 1$, adsorption is unfavorable.
- $R_L = 1$ indicates linearity of adsorption.
- In the case $R_L = 0$, adsorption is irreversible.

*2.5.2. Freundlich Adsorption Isotherm.* Freundlich claimed that adsorption takes place on surfaces with different adsorption energies and different characters. The amount of material adsorbed by the adsorbent ($q_e$) increases quickly with pressure or concentration and then shows a slow increase with filling of solid surface with adsorbed molecules. The variation of $q_e$ with pressure or concentration is given by the following equation according to the Freundlich model:[27]

$$q_e = K_f \cdot C_e^{\,1/n} \tag{11}$$

where $K_f$ (mg·g$^{-1}$) is a constant associated with adsorption capacity and $n$ is an empirical parameter associated with adsorption intensity and shows the strength of the interaction between the adsorbate and adsorbent. High $K_f$ values indicate


dx.doi.org/10.1021/je300597u | J. Chem. Eng. Data 2012, 57, 2733−2743

that the adsorbent and the adsorbate are very close to each other. The $n$ value changes with the heterogeneity of the adsorbate for the suitable adsorption process. Furthermore, the $n$ value for the adsorbent–adsorbate pair selected in terms of compatibility of adsorption should be between 1 and 10. The $1/n$ value is a heterogeneity factor and takes values in the range 0 to 1. The heterogeneity of the surface is an indication of how far $1/n$ value is away from zero.

In the Freundlich model, if the curvilinear equation above is rearranged and turned into linear form, the following new formula is obtained:

$$\ln q_e = \ln K_f + \frac{1}{n}\ln C_e \quad (12)$$

A $\ln C_e$–$\ln q_e$ graph comprises a line. $K_f$ and $1/n$ can be found from the intercept and slope of the line.

**2.6. Adsorption Thermodynamics.** The temperature dependency of adsorption is associated with the total energy change of the system ($\Delta H°$), usable Gibbs free energy change ($\Delta G°$), and energy change which is the criterion for entropy ($\Delta S°$). By these parameters, one can decide whether adsorption is a spontaneous process or not. In spontaneous chemical reactions and other physicochemical transformations free energy decreases; that is, standard $\Delta G°$ becomes negative. A positive $\Delta G°$ means free energy will increase. This shows that the reaction is progressing in the opposite direction, in other words, in the involuntary direction. The relationship among $\Delta H°$, $\Delta G°$, and $\Delta S°$ is as follows:

$$\Delta G° = \Delta H° - T\Delta S° \quad (13)$$

where $\Delta G°$ is the standard Gibbs free energy change ($kJ·mol^{-1}$), $\Delta H°$ is the standard enthalpy change ($kJ·mol^{-1}$), $\Delta S°$ is the standard entropy change ($kJ·mol^{-1}·K^{-1}$), $T$ is the absolute temperature (K), and $R$ is the universal gas constant ($8.314\ J·mol^{-1}·K^{-1}$).

To find Gibbs free energy of an adsorption procedure performed at a certain temperature, it is necessary to find equilibrium constant ($K_d$). $K_d$ is calculated by the ratio of amount of adsorbate adsorbed on unit mass of adsorbent to the amount remaining in the solution:

$$K_d = C_a/C_e \quad (14)$$

where $K_d$ is the adsorption equilibrium constant, $C_a$ is the adsorbate concentration adsorbed on unit mass of adsorbent ($mg·L^{-1}$), and $C_e$ is the adsorbate concentration remaining in the solution after adsorption ($mg·L^{-1}$).

$K_d$, found by the above equation, can be placed in the following equation, and the standard Gibbs free energy of adsorption can be obtained:

$$\Delta G° = -RT \ln K_d \quad (15)$$

Based on the equations above, the following van't Hoff equation can be derived:

$$\ln K_d = \frac{\Delta S°}{R} - \frac{\Delta H°}{RT} \quad (16)$$

A plot of $\ln K_d$ vs $1/T$ is a line. $\Delta H°$ and $\Delta S°$ values can be obtained from the slope and intercept, respectively. Thus, information about the progress of reaction can be achieved.[28]

A positive $\Delta H°$ shows that adsorption is endothermic, and a negative $\Delta H°$ shows that adsorption is exothermic. Furthermore, negative $\Delta G°$ values describe that adsorption is spontaneous. In other words, the applicability of the adsorption process can be understood from negative values of enthalpy and Gibbs free energy. Positive $\Delta S°$ values indicate an increase in randomness in the solid–solution interface.[29]

## 3. RESULTS AND DISCUSSION

**3.1. Characterization Results.** TIWAC obtained as a result of carbonization and activation procedures has significantly high carbon content (79.32 %) and extremely low ash content (1.04 %), as seen in Table 1. A C/H rate of 4 shows the increase in aromatization in activated carbon and, hence, formation of orderly structure and also transformation into a graphitical structure.

**Table 1. Characteristics of TIWAC**

| | |
|---|---|
| proximate analysis (wt %) | |
| moisture | 8.12 |
| volatile matter | 19.60 |
| ash | 1.04 |
| fixed carbon | 71.20 |
| carbon yield | 36.70 |
| ultimate (elemental) analysis (wt %) | |
| C | 79.32 |
| H | 1.79 |
| N | 3.45 |
| S | 0.24 |
| O[a] | 15.21 |
| C/H[b] | 3.72 |
| BET surface area ($m^2·g^{-1}$) | |
| $S_{BET}$ | 1066 |
| $S_{micro}$ | 641 |
| $S_{meso}$ | 425 |
| pore volume ($cm^3·g^{-1}$) | |
| $V_{total}$ | 0.580 |
| $V_{micro}$ | 0.337 |
| $V_{meso}$ | 0.243 |
| average pore diameter (nm) | |
| $D_p$ | 2.18 |
| iodine number ($mg·g^{-1}$) | 605.8 |
| methylene blue number ($mg·g^{-1}$) | 100.2 |

[a]By difference. [b]Mole ratio.

It is seen that the activated carbon has a structure of micromesoporous mixture with a significantly high BET surface area of 1066 $m^2·g^{-1}$. Therefore, it can be concluded that it may adsorb both small and large molecules (Table 1), which is also clear from the relatively high numbers of iodine and methylene blue.

SEM micrographs before phenol adsorption of TIWAC are given in Figure 1a,b, from which it is evident that TIWAC has a significantly porous structure. However, it is seen from Figure 1c,d that these pores have nearly disappeared after adsorption, suggesting that phenol molecules diffused toward the pores of TIWAC and, hence, were adsorbed.

Figure 2a,b shows IR spectra of TIWAC after and before phenol adsorption, respectively. In IR spectra taken before and after phenol adsorption, it is clear that functional groups appeared approximately at the same frequencies. When the spectrum before adsorption is considered, there are four noticeable peaks. The peak at 3372 $cm^{-1}$ indicates the –OH stretching vibration peak; the peaks at 2056 and 1543 $cm^{-1}$ indicate carboxylic acid and/or a lactone group, and the peak appearing at 1075 $cm^{-1}$ is the C–O stretching peak in


dx.doi.org/10.1021/je300597u | J. Chem. Eng. Data 2012, 57, 2733–2743

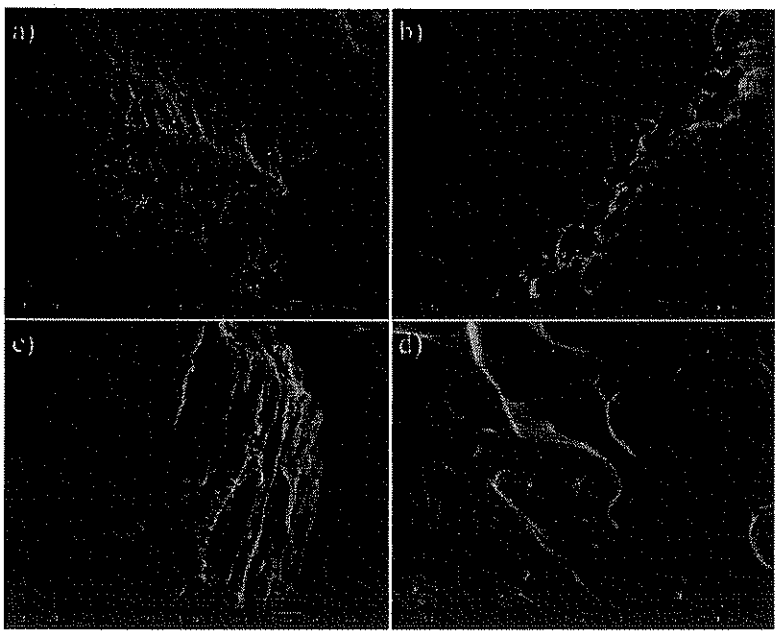


**Figure 1.** (a and b) SEM micrographs of TIWAC before phenol adsorption, magnified 500 and 1000 times, respectively, and (c and d) SEM micrographs of TIWAC magnified 1000 times after phenol adsorption.

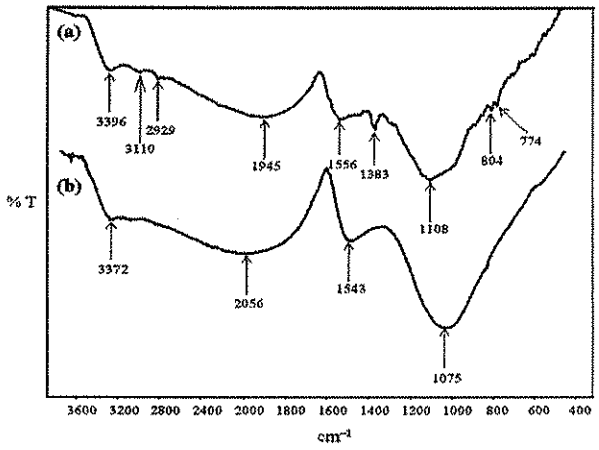


**Figure 2.** IR spectra for TIWAC (a) after and (b) before phenol adsorption.

heterocyclic rings. There are more peaks in the spectrum taken after phenol adsorption, and these peaks refer to phenol molecules. Hence, increasing transmittance and extra peaks arising from phenol molcules that have entered the structure indicate phenol adsorption from aqueous solution by activated carbon. Phenolic type C−H peaks appear at (3110 to 2929) $cm^{-1}$ in the spectrum taken after adsorption. The peak at 1383 $cm^{-1}$ indicates the existence of phenolic structure, and the peaks at (804 and 774) $cm^{-1}$ in the fingerprint area indicate a monosubstituted aromatic structure.[30]

**3.2. Effect of Initial pH on the Adsorption of Phenol by TIWAC.** Solution pH is one of the most important parameters influencing adsorption performance. The adsorption of organic materials on activated carbons, which is slightly different from metal adsorption, may take place with a higher yield in a much larger pH range. This result can be seen from the phenol adsorption graph plotted versus initial pH in Figure 3. It is apparent that, at low and high pH values, phenol adsorption on TIWAC is lower. In the light of this data, in this study, the optimum pH value was determined as 6.0.

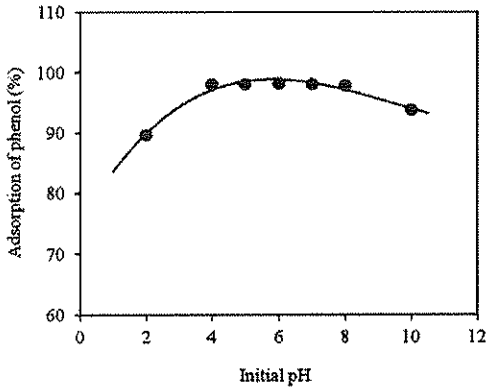


**Figure 3.** Effect of initial pH on the adsorption of phenol from aqueous solution by TIWAC (initial phenol conc.: 110 $mg \cdot L^{-1}$, TIWAC dose: 3.0 $g \cdot L^{-1}$, TIWAC particle size: < 150 $\mu m$, agitation time: 12 h).

The effects of pH on phenol adsorption were first studied by Snoeyink et al. (1969), and they also reported that phenol adsorption at low and high pH values is not favorable.[31] Since the $pK_a$ value of phenol is 9.89, the species which will be adsorbed at pH values above this value are mostly anionic. At high pH values, adsorbent surface and phenolate anions will distract each other because of the negativity of TIWAC surface, and hence, decreases in adsorption yield are observed. For low pH values, acidic solutions are used, which causes extra protons enter the solution. Since there will be a competition between protons and phenol for particularly carbonyl sites of activated


dx.doi.org/10.1021/je300597u | J. Chem. Eng. Data 2012, 57, 2733−2743

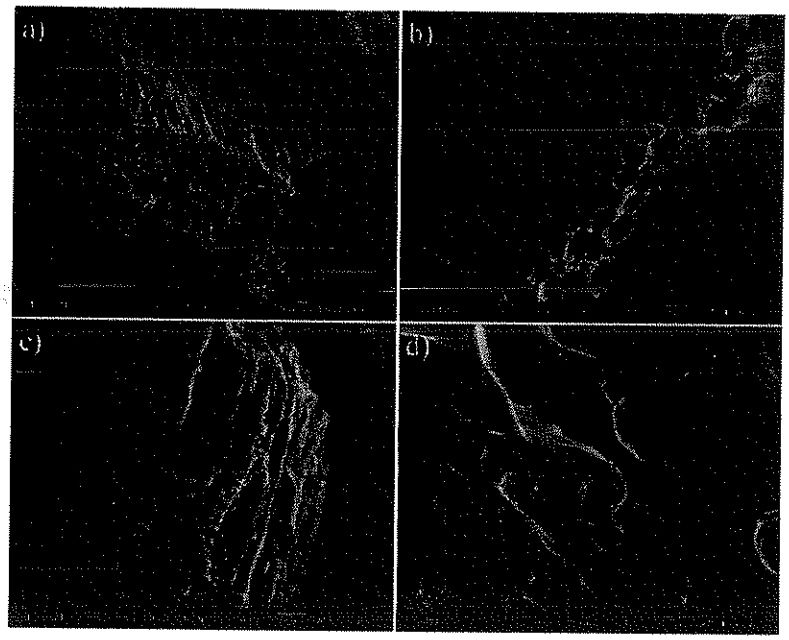


**Figure 1.** (a and b) SEM micrographs of TIWAC before phenol adsorption, magnified 500 and 1000 times, respectively, and (c and d) SEM micrographs of TIWAC magnified 1000 times after phenol adsorption.

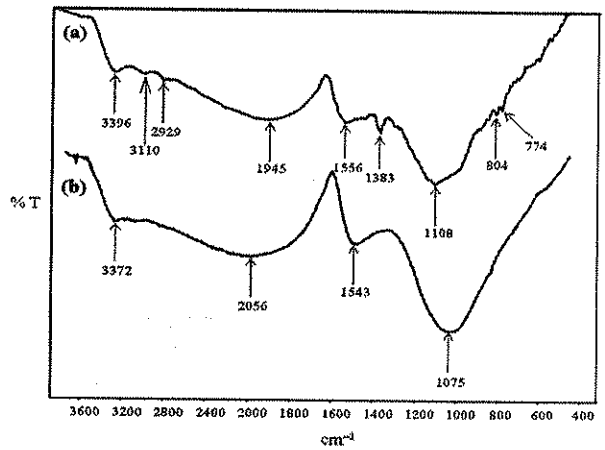


**Figure 2.** IR spectra for TIWAC (a) after and (b) before phenol adsorption.

heterocyclic rings. There are more peaks in the spectrum taken after phenol adsorption, and these peaks refer to phenol molecules. Hence, increasing transmittance and extra peaks arising from phenol molcules that have entered the structure indicate phenol adsorption from aqueous solution by activated carbon. Phenolic type C–H peaks appear at (3110 to 2929) $cm^{-1}$ in the spectrum taken after adsorption. The peak at 1383 $cm^{-1}$ indicates the existence of phenolic structure, and the peaks at (804 and 774) $cm^{-1}$ in the fingerprint area indicate a monosubstituted aromatic structure.[30]

**3.2. Effect of Initial pH on the Adsorption of Phenol by TIWAC.** Solution pH is one of the most important parameters influencing adsorption performance. The adsorption of organic materials on activated carbons, which is slightly different from metal adsorption, may take place with a higher yield in a much larger pH range. This result can be seen from the phenol adsorption graph plotted versus initial pH in Figure 3. It is apparent that, at low and high pH values, phenol adsorption on TIWAC is lower. In the light of this data, in this study, the optimum pH value was determined as 6.0.

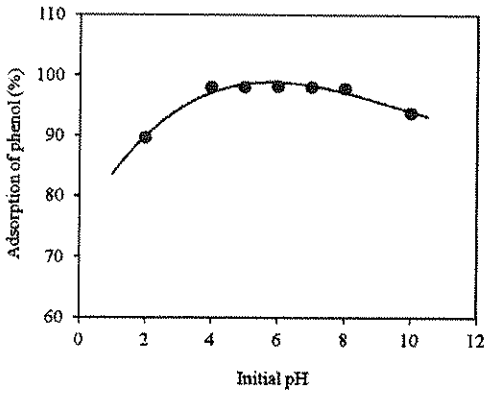


**Figure 3.** Effect of initial pH on the adsorption of phenol from aqueous solution by TIWAC (initial phenol conc.: 110 $mg \cdot L^{-1}$, TIWAC dose: 3.0 $g \cdot L^{-1}$, TIWAC particle size: < 150 $\mu m$, agitation time: 12 h).

The effects of pH on phenol adsorption were first studied by Snoeyink et al. (1969), and they also reported that phenol adsorption at low and high pH values is not favorable.[31] Since the $pK_a$ value of phenol is 9.89, the species which will be adsorbed at pH values above this value are mostly anionic. At high pH values, adsorbent surface and phenolate anions will distract each other because of the negativity of TIWAC surface, and hence, decreases in adsorption yield are observed. For low pH values, acidic solutions are used, which causes extra protons enter the solution. Since there will be a competition between protons and phenol for particularly carbonyl sites of activated


dx.doi.org/10.1021/je300597u | J. Chem. Eng. Data 2012, 57, 2733–2743

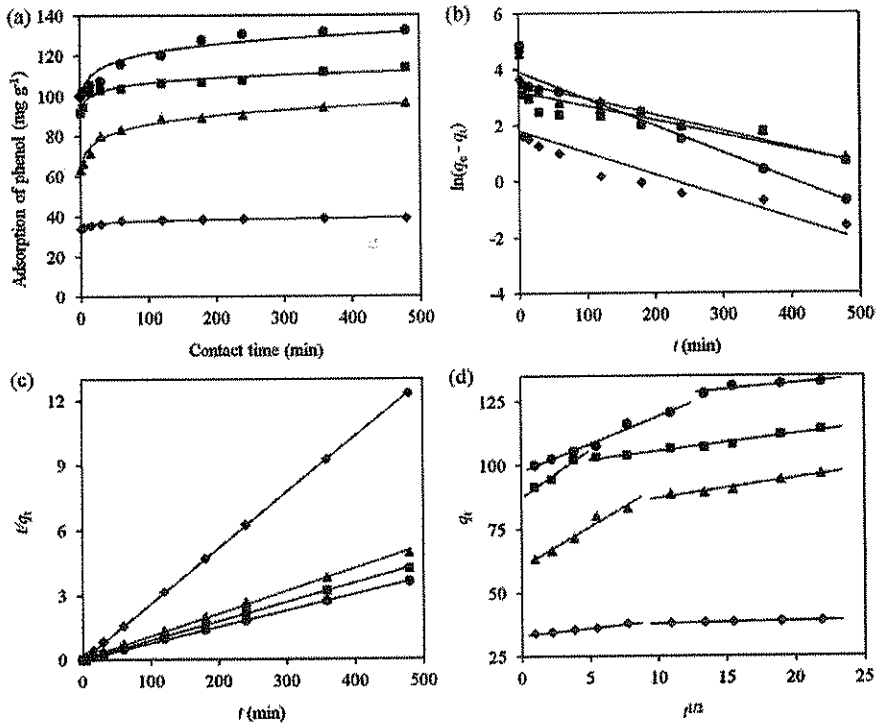


Figure 4. Adsorption kinetics of phenol from aqueous solution: (a) effect of contact time on phenol adsorption by TIWAC, (b) pseudofirst-order kinetic model of phenol adsorption, (c) pseudosecond-order kinetic model of phenol adsorption, (d) intraparticle diffusion model of phenol adsorption (initial pH: 6.0, initial phenol conc.: ◆, 100; ▲, 400; ■, 600, and ●, 1000 mg·L$^{-1}$, TIWAC dose: 2.0 g L$^{-1}$, TIWAC particle size: < 150 $\mu$m).

**Table 2. Constants of Kinetic Models for Phenol Adsorption on TIWAC**

| | | pseudofirst order | | | pseudosecond order | | | intraparticle diffusion | | |
|---|---|---|---|---|---|---|---|---|---|---|
| $C_o$ | $q_e$(exp.) | $q_e$(cal.) | $k_1$ | | $q_e$(cal.) | $k_2$ | | $k_{id}$ | C | |
| mg·L$^{-1}$ | mg·g$^{-1}$ | mg·g$^{-1}$ | min$^{-1}$ | $r^2$ | mg·g$^{-1}$ | g·mg$^{-1}$·min$^{-1}$ | $r^2$ | mg·g$^{-1}$·min$^{-1/2}$ | mg·g$^{-1}$ | $r^2$ |
| 100 | 39.0 | 6.1 | $-7.9\cdot10^{-3}$ | 0.7613 | 38.9 | $0.2\cdot10^{-3}$ | 0.9990 | 0.5657 | 33.3 | 0.9952 |
| 400 | 96.5 | 34.8 | $-5.9\cdot10^{-3}$ | 0.8385 | 95.2 | $2.2\cdot10^{-3}$ | 0.9985 | 3.1330 | 60.2 | 0.9660 |
| 600 | 114.0 | 24.9 | $-5.2\cdot10^{-3}$ | 0.6662 | 113.6 | $2.4\cdot10^{-3}$ | 0.9992 | 3.7036 | 87.2 | 0.9739 |
| 1000 | 132.5 | 51.4 | $-9.6\cdot10^{-3}$ | 0.9392 | 133.3 | $1.6\cdot10^{-3}$ | 0.9994 | 2.1416 | 97.5 | 0.9776 |

carbon, there will be a significant drop in adsorption yield at low pH values, as in Figure 3. In addition to these, the $pH_{pzc}$ value of TIWAC being 5.85 causes net charge of the adsorbent below this pH to be positive. Therefore, protonated species will repel each other, and thus, the adsorption yield will decrease. At pH 6.0, which was selected as the optimum, the net charge of the adsorbent is negative. Since phenol is still in the protonated position, adsorbate−adsorbent interactions will be maximum.[32]

**3.3. Effect of Contact Time and Adsorption Kinetics.** In terms of effectiveness and efficiency of adsorption process, completion of the process within a short time is extremely important for industrial applications. Figure 4a shows the effect of equilibrium time on the adsorption of phenol on TIWAC at four different initial concentrations in the range (100 to 1000) mg·L$^{-1}$. For four different concentrations of phenol, it is apparent that adsorption is very fast at the beginning and time to reach equilibrium increases with increasing concentration. For four concentrations, an agitation period of 4 h was determined as the optimum value in reaching equilibrium. Additionally, it can be seen that, during an agitation period of 8 h, the curve forms a flat plateau, and hence, within this period, adsorption of phenol on TIWAC indicates a monolayer adsorption process.

The adsorption kinetics of phenol on TIWAC was investigated by three different methods: pseudofirst-order, pseudosecond-order, and intraparticle diffusion.

For the first-order kinetic model, graphs of $\ln(q_e - q_t)$ versus $t$ and for second-order kinetic model graphs of $t/q_t$ versus $t$ were plotted (Figure 4b,c) with the obtained data and constants obtained for four different phenol concentrations given in Table 2. As can be seen from the table, when $r^2$ values are considered for four different phenol concentrations, the pseudosecond-order kinetic model represents the time-dependent function of equilibrium better than the pseudofirst-order kinetic model. Moreover, $q_e$(exp.) results are extremely compatible with $q_e$(cal.) values obtained by the second-order kinetic model. Therefore, the compatibility of systems reaching equilibrium with the pseudosecond-order kinetic model is also proven in this case.


dx.doi.org/10.1021/je300597u | J. Chem. Eng. Data 2012, 57, 2733−2743

To clarify the adsorption mechanism and determined rate-controlling step(s), the intraparticle diffusion model was applied to equilibrium data. Graphs of $q_t$ versus $t^{1/2}$ plotted for intraparticle diffusion show that the adsorption process essentially took place in two steps (Figure 4d). Within the first minute, a very fast adsorption takes place in the film layer on TIWAC surface. Then, intraparticle diffusion of phenol molecules toward the pores in inner surface of TIWAC starts, which indicates the migration of phenol molecules toward the sites where actual adsorption takes place. This step is thought to be the rate-determining or -limiting step. However, since none of $C$ constants obtained for intraparticle diffusion approach zero (Table 2), it emerges that adsorption rate is not only controlled by intraparticle diffusion. Therefore, the adsorption rate is controlled by film diffusion along with intraparticle diffusion.[33]

Table 3 shows the contribution of adsorption stages to adsorption at the end of adsorption process that has taken place

**Table 3. Contribution of Three Stages to Efficiency of Phenol Adsorption on TIWAC for the Intraparticle Diffusion Model**

| initial phenol conc. | contribution to adsorption efficiency (%) | | |
|---|---|---|---|
| $mg \cdot L^{-1}$ | film diffusion | intraparticle diffusion | equilibrium |
| 100 | 87.2 | 10.4 | 2.4 |
| 400 | 65.8 | 25.9 | 8.3 |
| 600 | 80.2 | 10.3 | 9.5 |
| 1000 | 75.5 | 21.1 | 3.4 |

in three stages being film diffusion on exterior surfaces, intraparticle diffusion toward the inside of pores, and equilibrium. The most important point that has to be considered here is that, for all concentrations, film diffusion was completed within the first minute at the end of a very fast process. Moreover, border layer diffusion (film diffusion) that has taken place within the first 1 min contributes the most to adsorption.

**3.4. Effect of TIWAC Dose on Adsorption of Phenol.** To study the effect of the amount of TIWAC on phenol adsorption, 10 mL portions from a phenol solution of 440 $mg \cdot L^{-1}$ under optimum conditions were individually treated with TIWAC in six different amounts ranging between (20 and 200) mg. A graph of phenol adsorption versus the amount of TIWAC was plotted from the data obtained (Figure 5). As seen from the figure, phenol adsorption percentage increased with an increasing amount of TIWAC, and a decrease in the amount of adsorbed phenol per gram of adsorbent was observed, which can be attributed to two reasons: (i) Increasing the amount of TIWAC against fixed phenol concentration causes the formation of surfaces who have not reached saturation on adsorbent surface. (ii) The adsorption capacity of TIWAC will be reduced since total surface area will be reduced as a result of clustering and agglomeration of a high amount of TIWAC particles.

If you look at the graph in Figure 5, you can see that phenol adsorption varied slightly after 80 mg of TIWAC. The phenol adsorption capacity of the adsorbent dosages used have realized as 53.2 % for 20 mg, 80.5 % for 40 mg, 95.5 % for 80 mg, 97.7 % for 100 mg, 98.6 % for 150 mg, and 99.5 % for 200 mg, respectively.

**3.5. Effect of Initial Phenol Concentration and Adsorption Isotherms.** To study the effect of initial phenol

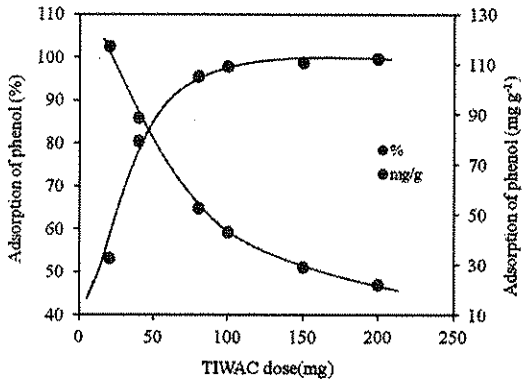


**Figure 5.** Effect of TIWAC dose on adsorption of phenol (initial phenol conc.: 440 $mg \cdot L^{-1}$, initial pH: 6.0, TIWAC doses: (20 to 200) mg, TIWAC particle size: < 150 $\mu$m, agitation time: 4.0 h).

concentration ($C_o$) on phenol adsorption on TIWAC, a fixed TIWAC dosage of 2.0 $g \cdot L^{-1}$ was treated with phenol solutions with concentrations ranging between (90 and 960) $mg \cdot L^{-1}$ under optimum conditions. As seen from the graph of $C_o - q_e$ in Figure 6, increasing the initial phenol concentration versus the

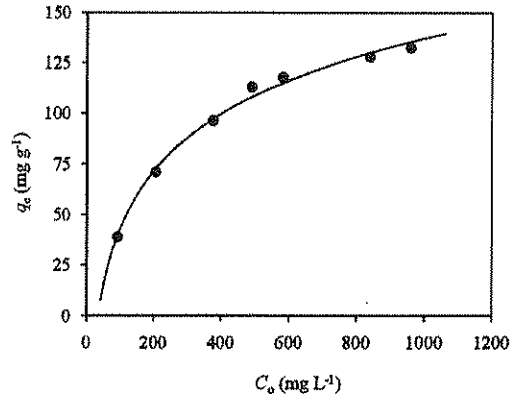


**Figure 6.** Effect of initial phenol concentration on the adsorption of phenol by TIWAC (initial pH: 6.0, initial phenol conc.: (90 to 960) $mg \cdot L^{-1}$, TIWAC dose: 2.0 $g \cdot L^{-1}$, TIWAC particle size: < 150 $\mu$m, agitation time: 4.0 h).

amount of phenol adsorbed on the adsorbent shows a nonlinear increase. Increasing phenol concentration is an impact increasing the capacity of the fixed amount of adsorbent. Furthermore, increasing $C_o$ causes adsorbate–adsorbent interaction to increase more. A further increase in $C_o$ causes the adsorbent reach saturation, and thus the capacity of adsorbent is determined.[34]

The relation between the phenol concentration remained unadsorbed in the solution at equilibrium ($C_e$), and the amount of phenol adsorbed on the adsorbent ($q_e$) is examined by adsorption isotherms. In this study, the equilibrium established between phenol and TIWAC in aqueous solution was described by Langmuir and Freundlich isotherm models. A graph of $C_e$ versus $q_e$ is widely used in the derivation of various isotherms and interpretation of data (Figure 7a). Figure 7b,d shows a linear Langmuir graph and a linear Freundlich graph, respectively. When correlation coefficients ($r^2$) of the graphs are considered, it is apparent that they are very high. Therefore,


dx.doi.org/10.1021/je300597u | J. Chem. Eng. Data 2012, 57, 2733–2743

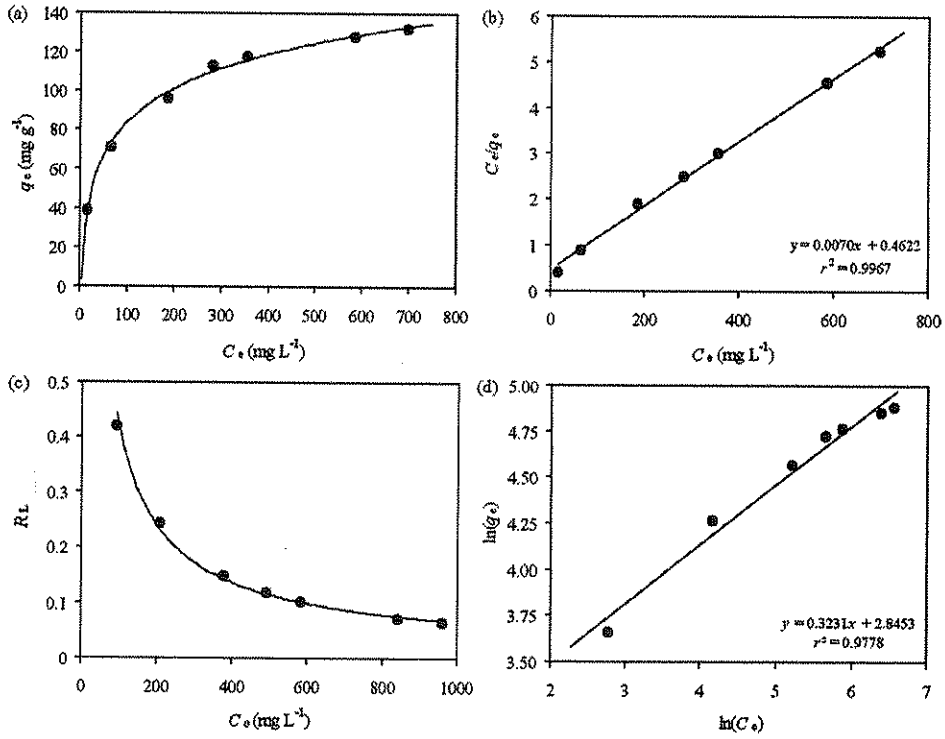


Figure 7. Relationship between phenol molecules at equilibrium and phenol molecules adsorbed on TIWAC: (a) $C_e$ versus $q_e$ graph, (b) linear Langmuir isotherm graph; $C_e$ versus $C_e/q_e$ graph, (c) $R_L$ versus $C_o$ graph, (d) linear Freundlich isotherm graph; ln($C_e$) versus ln($q_e$) graph.

**Table 4. Constants of Langmuir and Freundlich Isotherms for the Adsorption of Phenol on TIWAC**

| | Langmuir constants | | | | | Freundlich constants | | | |
|---|---|---|---|---|---|---|---|---|---|
| TIWAC dose | $q_{max}$ | | b | | | $K_f$ | | | |
| g L$^{-1}$ | mmol·g$^{-1}$ | mg·g$^{-1}$ | L·mmol$^{-1}$ | L·mg$^{-1}$ | $r^2$ | mmol·g$^{-1}$ | mg·g$^{-1}$ | $n$ | $r^2$ |
| 2.0 | 1.52 | 142.9 | 1.421 | $1.51 \cdot 10^{-2}$ | 0.9967 | 0.1828 | 17.207 | 3.095 | 0.9778 |

the adsorption of phenol on TIWAC in aqueous solution follows both of these isotherm models. $R_L$ which is a parameter of Langmuir isotherm also determines the conformance of adsorption to the selected adsorbate–adsorbent system. In the case of the $R_L$–$C_o$ graph (Figure 7c), all $R_L$ values under 1 show that phenol adsorption on TIWAC is extremely favorable.

Constants obtained from Langmuir and Freundlich isotherms are given in Table 4. By the courtesy of the Langmuir isotherm model, the maximum adsorption capacity ($q_{max}$) of any adsorbent for a specific adsorbate can be determined. Phenol adsorption capacity of TIWAC against an amount of 2.0 g L$^{-1}$ was calculated as 142.9 mg·g$^{-1}$ (1.52 mmol·g$^{-1}$). If this value is relatively compared to the values reported by other studies in the literature, it is seen that this value is higher than many such values (Table 5).

To better understand with which isotherm model the data can be defined better, Langmuir and Freundlich isotherm curves can be utilized. For this purpose, if constants obtained from linear graphs are put in place in the equations used for plotting curve forms, graphs of $C_e$–$q_e$ of each model can be rederived as in Figure 8. Since the empirical points are better represented by Langmuir graph, it is apparent that our data better follows the Langmuir isotherm model. Hence, it can be concluded that TIWAC has a homogeneous surface during phenol adsorption.

**Table 5. Comparison of Langmuir Adsorption Capacity ($q_{max}$) of TIWAC for Phenol, with Other Adsorbents in the Literature [$T$: (20 to 30) °C]**

| | | adsorbent dosage | $q_{max}$ | |
|---|---|---|---|---|
| adsorbent | particle size (μm) | g·L$^{-1}$ | mg·g$^{-1}$ | ref. |
| bagasse fly ash | – | 10.0 | 23.331 | 34 |
| AC fibers | – | 1.0 | 102.5 | 35 |
| coconut shells, AC | 74 to 595[a] | 1.0 | 49.87 | 36 |
| rattan sawdust | 150 | 1.0 | 149.25 | 37 |
| vetiver roots, AC | – | 0.4 | 145 | 38 |
| date pits, AC | 125 to 212 | 5.0 | 46.076 | 39 |
| granular AC | 3000 | 0.6 | 238.09 | 40 |
| *Tectona grandis* sawdust, AC | 150 to 200 | 5.0 | 13.45 | 41 |
| clay | 50 | 4.0 | 40.121 | 42 |
| commercial granular AC | 150 to 250 | 1.0 | 74.12 | 43 |
| TIWAC | <150 | 2.0 | 142.9 | This work |

[a]Reported as (30 to 200) mesh. – indicates not reported. AC: activated carbon.


dx.doi.org/10.1021/je300597u | J. Chem. Eng. Data 2012, 57, 2733–2743

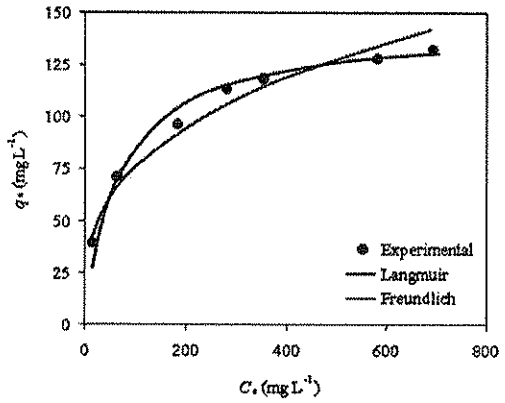


Figure 8. Nonlinear Langmuir–Freundlich isotherm graphs.

**3.6. Effect of Temperature on the Adsorption of Phenol and Adsorption Thermodynamics.** To study the effect of temperature on phenol adsorption on TIWAC, a series of phenol solutions with a concentration of 100 mg·L$^{-1}$ and pH of 6 at various temperatures ranging between (0 and 40) °C were treated with 2.0 g·L$^{-1}$ of TIWAC for 4.0 h. If you look at the temperature–phenol adsorption graph in Figure 9a, you can see that adsorption efficiency decreased with increasing temperature, suggesting that phenol adsorption on TIWAC has an exothermic nature. A negative effect of temperature on phenol adsorption on various adsorbents has been reported by many studies.

The temperature increase especially causes effects on the chemistry of carbon surfaces. An increase is observed on the water adsorption capacity of porous carbons with increasing temperature. In addition, changes also take place in hydration grades of species dissolved in aqueous solution. The interaction energy of phenol–water changes with increasing temperature and water adsorption by the carbon greatly modifies the phenol adsorption mechanism. Therefore, since a significant portion of active sites are occupied by water molecules, they will weaken $\pi$–$\pi$ interactions, which are primary bonding mechanisms of phenol on activated carbon and the donor–acceptor complex formations.[32]

In the case of phenol adsorption, which advances through donor–acceptor formation, primary active groups are carbonyl and basic groups. Since temperature increase will cause a decrease in the efficiency of these groups, the adsorption capacity of the relevant adsorbent will only be limited by the microporous structure.[44]

Thermodynamic parameters can be determined by the courtesy of a phenol adsorption graph plotted as a function of temperature. $\Delta G$, $\Delta S$, and $\Delta H$ values were determined from a graph of ln $K_d$ versus $1/T$ (Figure 9b). It is seen in Table 6

**Table 6. Thermodynamic Parameters of Phenol Adsorption on TIWAC at Different Temperature**

| T (°C) | $K_d$ | $\Delta G$ (kJ mol$^{-1}$) | $\Delta S$ (J mol$^{-1}$ K$^{-1}$) | $\Delta H$ (kJ mol$^{-1}$) |
|---|---|---|---|---|
| 0 | 6.69 | −4.31 | | |
| 10 | 6.14 | −4.27 | | |
| 20 | 5.67 | −4.23 | 0.36 | −4.38 |
| 30 | 5.41 | −4.25 | | |
| 40 | 5.25 | −4.32 | | |

that all $\Delta G$ values are negative, suggesting that phenol adsorption on TIWAC takes place spontaneously. A $\Delta H$ value of −4.38 shows that the reaction is exothermic and the adsorption advances primarily by physical means.

**3.7. Salt Effect on the Adsorption of Phenol by TIWAC.** To study the effects of various salts on phenol adsorption on TIWAC (ionic strength), individual KCl, $Na_2SO_4$, and $NaNO_3$ salts with concentrations ranging between (0 and 0.20) mol·L$^{-1}$ were treated with phenol solutions of 105 mg·L$^{-1}$. The graph in Figure 10 shows that the adsorption of

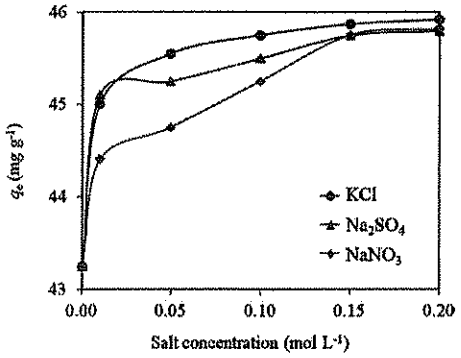


Figure 10. Effect of some salts on the adsorption of phenol by TIWAC [initial pH: 6.0, each salt conc.: (0 and 0.20) mol·L$^{-1}$, phenol conc.: 105 mg·L$^{-1}$, TIWAC dose: 2.0 g·L$^{-1}$, TIWAC particle size: < 150 $\mu$m, agitation time: 4.0 h].

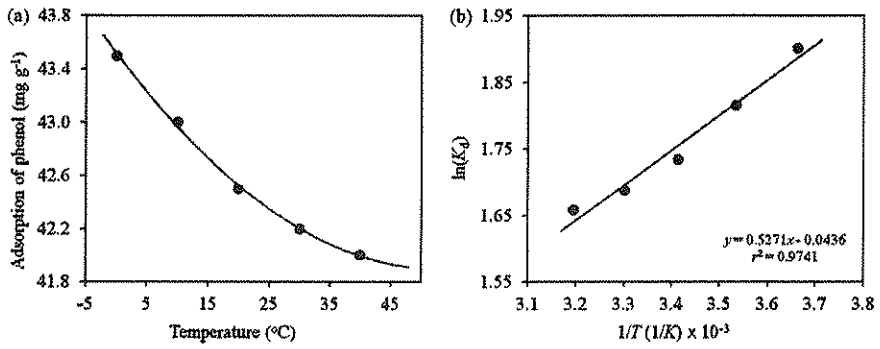


Figure 9. (a) Effect of temperature on the adsorption of phenol by TIWAC, (b) ln($K_d$) versus $1/T$ graph for thermodynamic parameters (initial phenol conc.: 100 mg·L$^{-1}$, initial pH: 6.0, TIWAC particle size: < 150 $\mu$m, agitation time: 4.0 h).


dx.doi.org/10.1021/je300597u | J. Chem. Eng. Data 2012, 57, 2733–2743

phenol on TIWAC increases with increasing ionic strength of the medium. The adsorption efficiency which was 83.2 % in distilled water medium increased to 88.3 % in the presence of KCl ranging between (0 and 0.20) mol·L$^{-1}$ and to 88.1 % in the presence of $Na_2SO_4$ and $NaNO_3$.

During adsorbate−adsorbent interaction in aqueous solution, an electrical double-layer arising from electrostatic interactions is formed in the interface.[45] A slight increase in phenol adsorption with increasing ionic strength arises from the oppression of the double-layer. The effect of ionic strength can also be described by electrostatic interactions, which are in the form of pulling or pushing. Salt which is added to the medium increases the ionic strength of the solution and reduces these effects. This situation arises from the shielding effect of surface charge generated by the salt. If the electrostatic interaction between adsorbent surface and adsorbate molecules is in the form of pushing or surface concentration is saturated sufficiently, any increase in ionic strength will increase adsorption. Phenol adsorption on TIWAC increased with increasing ionic strength. At pH 6.0, the surface charge of the adsorbent is negative. Salt added to the medium has shielded surface charge with the increase in electrolyte concentration.[46]

The presence of electrolytes in the solution decreases the solubility of phenol in aqueous solution and shows an effect known as salting-out in the literature. Thus, this effect facilitates adsorption of phenol on activated carbon. Consequently, the presence of electrolytes in aqueous solution is extremely efficient in increasing the phenol adsorption capacity of the activated carbon.[47]

## 4. CONCLUSIONS

From the data obtained, it is seen that phenol adsorption capacity of TIWAC (142.9 mg·g$^{-1}$) is significantly good and much higher than many other activated carbons reported in the literature (Table 5). This result particularly shows that a waste material which is of no use and has a potential to cause environmental pollution (tea industry waste) has turned into an extremely beneficial material. The feasibility of obtaining high performance activated carbons from agricultural waste materials at very low costs gradually increases the number of studies carried out in this field.

Some of the results obtained as a result of various analytical procedures carried out for phenol adsorption on TIWAC can be listed as follows:

- The ability of TIWAC to adsorb phenol ions from aqueous solution have been realized in a wide pH range. In very acidic and very basic regions, the efficiency of adsorption is slightly reduced.
- In the case of kinetics studies carried out with four different initial concentrations, the maximum adsorption efficiency was reached in a minimum of 4.0 h. It was understood that phenol adsorption on TIWAC followed pseudosecond-order kinetic model better and the adsorption rate is controlled by both boundary layer diffusion and intraparticle diffusion.
- The percentage of phenol adsorption was showing a nonlinear increase with an increasing amount of TIWAC, whereas a decrease was observed in the amount of phenol adsorbed per grams of adsorbent.
- From the adsorption graphs plotted as a result of increasing phenol concentration at fixed amount of TIWAC, it was seen that the adsorption behavior of TIWAC is better described by the Langmuir adsorption model, rather than the Freundlich model. It was also established that the phenol adsorption capacity of TIWAC is significantly high compared to those values in the literature.
- As in the case of many studies in the literature, an increase in temperature lowered phenol adsorption on TIWAC. Therefore, it is apparent that adsorption behavior is exothermic, which is also verified by the negative $\Delta H$ value −4.38 kJ·mol$^{-1}$, thereby supporting the fact that the adsorption in question primarily took place by physical means. Negative $\Delta G$ values indicate that adsorption took place spontaneously.
- As in the case of adsorption of other organic molecules on various adsorbents, it was seen that ionic strength had a positive effect on phenol adsorption on TIWAC. An increase was also observed in phenol adsorption with an increasing amount of various electrolytes in the medium.

## AUTHOR INFORMATION


### Corresponding Author

*E-mail: a.ramazan.gundogdu@gmail.com. Tel.: +90 462 377 2498. Fax: +90 462 3253196.



### Funding

Authors would like to thank the Unit of the Scientific Research Projects of Karadeniz Technical University for the financial support via the project 2008.111.002.1.


### Notes

The authors declare no competing financial interest.

## ACKNOWLEDGMENTS


The authors would like to thank the Central Laboratory of Middle East Technical University, Ankara, Turkey for surface characterization analyses of the adsorbents and TUBITAK Marmara Research Center, Kocaeli, Turkey for SEM analyses. The authors also thank Dr. Yaprak Asamaz and Dr. Yunus Onal for their contributions.


## REFERENCES


(1) Callega, G.; Serna, J.; Rodriguez, J. Kinetics of Adsorption of Phenolic Compounds from Wastewater onto Activated Carbon. *Carbon* **1993**, *31*, 691−697.

(2) Singh, B. K.; Rawat, N. S. Comparative Sorption Kinetic Studies of Phenolic Compounds on Fly Ash and Impregnated Fly Ash. *J. Chem. Technol. Biotechnol.* **1994**, *61*, 57−65.

(3) Lee, J. H.; Song, D. I.; Jeon, W. Y. Adsorption of Organic Phenols onto Dual Organic Cation Montmorillionite from Water. *Sep. Sci. Technol.* **1997**, *32*, 1975−1992.

(4) Bulbul, G.; Aksu, Z. Investigation of Wastewater Treatment Containing Phenol Using Fee and Ca-Alginate Gel Immobilized P. putida in a Batch Stirred Reactor. *Turk. J. Eng. Environ. Sci.* **1997**, *21*, 175−181.

(5) Tailor, R.; Shah, B.; Shah, A. Sorptive Removal of Phenol by Zeolitic Bagasse Fly Ash: Equilibrium, Kinetics, and Column Studies. *J. Chem. Eng. Data* **2012**, *57*, 1437−1448.

(6) Senturk, H. B.; Ozdes, D.; Gundogdu, A.; Duran, C.; Soylak, M. Removal of Phenol from Aqueous Solutions by Adsorption onto Organomodified Tirebolu Bentonite: Equilibrium, Kinetic and Thermodynamic Study. *J. Hazard. Mater.* **2009**, *172*, 353−362.

(7) Ioannidou, O.; Zabaniotou, A. Agricultural Residues as Precursors for Activated Carbon Production−A Review. *Renewable Sustainable Energy Rev.* **2007**, *11*, 1966−2005.

(8) Paraskeva, P.; Kalderis, D.; Diamadopoulos, E. Production of Activated Carbon from Agricultural By-products. *J. Chem. Technol. Biotechnol.* **2008**, *83*, 581−592.
(9) Dias, J. M.; Alvim-Ferraz, M. C.; Almeida, M. F.; Rivera-Utrilla, J.; Sanchez-Polo, M. Waste Materials for Activated Carbon Preparation and its Use in Aqueous-Phase Treatment: A Review. *J. Environ. Manage.* **2007**, *85*, 833−846.
(10) Radeke, K. H.; Loseh, D.; Struve, K.; Weiss, E. Comparing Adsorption of Phenol from Aqueous Solution onto Silica Fangasite, Activated Carbon and Polymeric Resin. *Zeolites* **1993**, *13*, 69−70.
(11) Anirudhan, T. S.; Sreekumari, S. S.; Brigle, C. D. Removal of Phenols from Water and Petroleum Industry Refinery Effluents by Activated Carbon Obtained from Coconut Coir Pith. *Adsorption* **2009**, *15*, 439−451.
(12) Imamoğlu, M.; Tekir, O. Removal of Copper (II) and Lead (II) Ions from Aqueous Solutions by Adsorption on Activated Carbon from a New Precursor Hazelnut Husks. *Desalination* **2008**, *228*, 108−113.
(13) Teker, M.; Imamoglu, M.; Saltabas, O. Adsorption of Copper and Cadmium Ions by Activated Carbon from Rice Hulls. *Turk. J. Chem.* **1999**, *23*, 185−191.
(14) Onal, Y.; Akmil-Basar, C.; Sarıcı-Ozdemir, C.; Erdogan, S. Textural Development of Sugar Beet Bagasse Activated with $ZnCl_2$. *J. Hazard. Mater.* **2007**, *142*, 138−143.
(15) ASTM D2854-96(2004), *Standard Test Method for Total Ash Content of Activated Carbon*; Annual Book of ASTM Standards; ASTM: West Conshohocken, PA, 2006.
(16) ASTM D5832-98(2003), *Standard Test Method for Volatile Matter Content of Activated Carbon Samples*; Annual Book of ASTM Standards; ASTM: West Conshohocken, PA, 2006.
(17) Raposo, F.; De La Rubia, M. A.; Borja, R. Methylene Blue Number as Useful Indicator to Evaluate the Adsorptive Capacity of Granular Activated Carbon in Batch Mode: Influence of Adsorbate/Adsorbent Mass Ratio and Particle Size. *J. Hazard. Mater.* **2009**, *165*, 291−299.
(18) ASTM D4607-94(1999), *Standard Test Method for Determination of Iodine Number of Activated Carbon*; Annual Book of ASTM Standards; ASTM: West Conshohocken, PA, 2006.
(19) Lagergren, S. About the Theory of So-Called Adsorption of Soluble Substance. *Kungl. Sven. Veterskopsakad. Handl.* **1898**, *24*, 1−39.
(20) Yavuz, O.; Altunkaynak, Y.; Guzel, F. Removal of Copper, Nickel, Cobalt and Manganese from Aqueous Solution by Kaolinite. *Water Res.* **2003**, *37*, 948−952.
(21) Ho, Y. S.; McKay, G. Kinetic Models for the Sorption of Dye from Aqueous Solution by Wood. *Process Saf. Environ. Protect.* **1998**, *76*, 183−191.
(22) Weber, W. J.; Morris, J. C. Kinetics of Adsorption on Carbon from Solution. *J. Sanit. Eng. Div. Am. Soc. Civ. Eng.* **1963**, *89*, 31−59.
(23) Mall, I. D.; Srivastava, V. C.; Agarwal, N. K.; Mishra, I. M. Removal of Congo Red from Aqueous Solution by Bagasse Fly Ash and Activated Carbon: Kinetic Study and Equilibrium Isotherm Analyses. *Chemosphere* **2005**, *61*, 492−501.
(24) Gupta, G. S.; Prasad, G.; Singh, V. N. Removal of Chrome Dye from Aqueous Solutions by Mixed Adsorbents: Fly Ash and Coal. *Water Res.* **1990**, *24*, 45−50.
(25) Langmuir, I. The Adsorption of Gases on Plane Surfaces of Glass, Mica, and Platinum. *J. Am. Chem. Soc.* **1918**, *40*, 1361−1403.
(26) Hall, K. R.; Eagleton, L. C.; Acrivos, A.; Vermeulen, T. Pore and Solid-Diffusion Kinetics in Fixed-Bed Adsorption Under Constant-Pattern Conditions. *Ind. Eng. Chem. Fundam.* **1966**, *5*, 212−223.
(27) Freundlich, H. M. F. Über die Adsorption in Lösungen. *Z. Phys. Chem.* **1906**, *57*, 385−470.
(28) Amana, T.; Kazi, A. A.; Sabri, M. U.; Banoa, Q. Potato Peels as Solid Waste for the Removal of Heavy Metal Copper(II) from Waste Water/Industrial Effluent. *Colloids Surf., B* **2008**, *63*, 116−121.
(29) Atkins, P.; de Paula, J. *Physical Chemistry*, 8th ed.; Oxford University Press: Oxford, U.K., 2006.
(30) Stuart, B. H. *Infrared Spectroscopy: Fundamentals and Applications*; John Wiley & Sons: West Sussex, 2004.
(31) Snoeyink, V. L.; Weber, W. J., Jr.; Mark, H. B. Sorption of Phenol and Nitrophenol by Active Carbon. *Environ. Sci. Technol.* **1969**, *3*, 918−926.
(32) Dabrowski, A.; Podkoscielny, P.; Hubicki, Z.; Barczak, M. Adsorption of Phenolic Compounds by Activated Carbon—a Critical Review. *Chemosphere* **2005**, *58*, 1049−1070.
(33) Ofomaja, A. E. Kinetics and Mechanism of Methylene Blue Sorption onto Palm Kernel Fibre. *Process Biochem.* **2007**, *42*, 16−24.
(34) Srivastava, V. C.; Swamy, M. M.; Mall, I. D.; Prasad, B.; Mishra, I. M. Adsorptive Removal of Phenol by Bagasse Fly Ash and Activated Carbon: Equilibrium, Kinetics and Thermodynamics. *Colloids Surf.: Physicochem. Eng. Aspects* **2006**, *272*, 89−104.
(35) Liu, Q. S.; Zheng, T.; Wang, P.; Jiang, J. P.; Li, N. Adsorption Isotherm, Kinetic and Mechanism Studies of Some Substituted Phenols on Activated Carbon Fibers. *Chem. Eng. J.* **2010**, *157*, 348−356.
(36) Singh, K. P.; Malik, A.; Sinha, S.; Ojha, P. Liquid-Phase Adsorption of Phenols Using Activated Carbons Derived from Agricultural Waste Material. *J. Hazard. Mater.* **2008**, *150*, 626−641.
(37) Hameed, B. H.; Rahman, A. A. Removal of Phenol from Aqueous Solutions by Adsorption onto Activated Carbon Prepared from Biomass Material. *J. Hazard. Mater.* **2008**, *160*, 576−581.
(38) Altenor, S.; Carene, B.; Emmanuel, E.; Lambert, J.; Ehrhardt, J. J.; Gaspard, S. Adsorption Studies of Methylene Blue and Phenol onto Vetiver Roots Activated Carbon Prepared by Chemical Activation. *J. Hazard. Mater.* **2009**, *165*, 1029−1039.
(39) Banat, F.; Al-Asheh, S.; Al-Makhadmeh, L. Utilization of Raw and Activated Date Pits for the Removal of Phenol from Aqueous Solutions. *Chem. Eng. Technol.* **2004**, *24*, 80−86.
(40) Hamdaoui, O.; Naffrechoux, E. Modeling of Adsorption Isotherms of Phenol and Chlorophenols onto Granular Activated Carbon: Part I. Two-Parameter Models and Equations Allowing Determination of Thermodynamic Parameters. *J. Hazard. Mater.* **2007**, *147*, 381−394.
(41) Mohantya, K.; Dasb, D.; Biswas, M. N. Adsorption of Phenol from Aqueous Solutions Using Activated Carbons Prepared from Tectona Grandis Sawdust by $ZnCl_2$ Activation. *Chem. Eng. J.* **2005**, *115*, 121−131.
(42) Nayak, P. S.; Singh, B. K.; Nayak, S. Equilibrium, Kinetic and Thermodynamic Studies on Phenol Sorption to Clay. *J. Environ. Protect. Sci.* **2007**, *1*, 83−91.
(43) Vasu, A. E. Removal of Phenol and o-Cresol by Adsorption onto Activated Carbon. *E-J. Chem.* **2008**, *5*, 224−232.
(44) Terzyk, A. P. Further Insights into the Role of Carbon Surface Functionalities in the Mechanism of Phenol Adsorption. *J. Colloid Interface Sci.* **2003**, *268*, 301−329.
(45) Osipow, L. I. *Surface Chemistry: Theory and Industrial Applications*; Krieger: New York, 1972.
(46) Castilla, C. M. Adsorption of Organic Molecules from Aqueous Solutions on Carbon Materials. *Carbon* **2004**, *42*, 83−94.
(47) Tan, I. A. W.; Ahmad, A. L.; Hameed, B. H. Adsorption of basic dye on high-surface-area activated carbon prepared from coconut husk: Equilibrium, kinetic and thermodynamic studies. *J. Hazard. Mater.* **2008**, *154*, 337−346.